Dissociative Route to C−H Bond Activation: DFT Study of Ligand Cyclometalation in a Platinum(II) Complex

Alessandro Marrone,[†] Nazzareno Re,*[,†] and Raffaello Romeo*[,‡]

Dipartimento di Scienze del Farmaco, Università G. d'Annunzio, Via dei Vestini 31, 66100 Chieti, Italy, and Dipartimento di Chimica Inorganica, Chimica Analitica e Chimica Fisica, Università di Messina, Salita Sperone 31, Vill. S. Agata, 98166 Messina, Italy

Received October 24, 2007

Density functional calculations have been carried out on the cycloplatination reaction of *cis*-[Pt(Me)$_2$(dmso)(P(*o*-tol)$_3$)] (**1**) leading to the C,P-cyclometalated compound [Pt{CH$_2$C$_6$H$_4$P(*o*-tolyl)$_2$-κC,*P*}(Me)(dmso)] (**6**) with liberation of methane. Our calculations have confirmed that this reaction develops along a multistep mechanism consisting of (i) reversible dissociation of the dmso ligand to give the coordinatively unsaturated 14-electron T-shaped intermediate [Pt(Me)$_2$(P(*o*-tol)$_3$)] (**2**), (ii) intramolecular oxidative addition of the C−H bond of a methyl group on the P(*o*-tol)$_3$ ligand to give the pentacordinate cyclometalated hydride species **3**, (iii) reductive elimination of methane to give the σ-complex **4**, which evolves to the unsaturated 14-electron species **5**, and (iv) fast reassociation of the dmso ligand to give the final C,P-cyclometalated square-planar product **6**, allowing also for an evaluation of the energies and a better understanding of the bonding and structural features of the species intercepted along the potential energy surface (PES) of the reaction.

Introduction

Understanding and developing efficient methods for selective carbon−hydrogen bond activation and functionalization is a longstanding and current target in organic and organometallic chemistry.[1] In this context, cyclometalation reactions represent examples of intramolecular C−H bond activation mediated by transition metals.[2] The interest in cyclometalated compounds is further encouraged by their manifold application as reagents or catalysts for important organic transformations, such as the synthesis of heterocyclic compounds,[3] carbon−carbon bond-forming reactions,[4] and alkane dehydrogenation,[5] and by their attractive photochemical and photophysical properties,[6] as well as for their potential use as molecular devices.[7] Several examples of cyclometalated complexes can be found in platinum(II) chemistry.[8] We have demonstrated, however, that in some of these versatile compounds cycloplatination does not play any particular role in controlling rates and mechanisms of ligand substitution reactions.[9]

In the search for new synthetic procedures to circumvent the kinetic inertness of 16-electron square-planar complexes toward C−H activation, we planned to use electron-rich compounds,

* To whom correspondence should be addressed. N.R.: tel, +39 0871 3554603; fax, +39 0871 3554614; e-mail, nre@unich.it. R.R.: tel, +39 090 6765717; fax, +39 090 393756; e-mail, rromeo@unime.it.

† Università G. d'Annunzio.

‡ Università di Messina.

(1) A representative, but not comprehensive, list of reviews on C−H activation and functionalization includes: (a) Bergman, R. G. *Nature* **2007**, *446*, 391–393. (b) Labinger, J. A.; Bercaw, J. E. *Nature* **2002**, *417*, 507–514. (c) Arndtsen, B. A.; Bergman, R. G.; Mobley, T. A.; Peterson, T. H. *Acc. Chem. Res.* **1995**, *28*, 154–162. (d) Shilov, A. E.; Shul'pin, G. B. *Chem. Rev.* **1997**, *97*, 2879–2932. (e) Erker, G. *Angew. Chem., Int. Ed.* **1999**, *38*, 1699–1712. (f) Davies, H. M. L.; Antoulinakis, E. G. *J. Organomet. Chem.* **2001**, *617–618*, 47–55. (g) Crabtree, R. H. *Dalton Trans.* **2001**, *17*, 2437–2450. (h) Fekl, U.; Goldberg, K. I. *Adv. Inorg. Chem.* **2003**, *54*, 259–320.

(2) For recent reviews on cyclometalation, see: (a) Crabtree, R. H. *J. Organomet. Chem.* **2005**, *690*, 5451–5457. (b) Slagt, M. Q.; van Zwieten, D. A. P.; Moerkerk, A. J. C. M.; Gebbink, R. J. M. K.; van Koten, G. *Coord. Chem. Rev.* **2004**, *248*, 2275–2282. (c) Omae, I. *Coord. Chem. Rev.* **2004**, *248*, 995–1023. (d) Werner, H. *Dalton Trans.* **2003**, *20*, 3829–3837. (e) Ryabov, A. D. *Chem. Rev.* **1990**, *90*, 403–424. (f) Newkome, G. R.; Puckett, W. E.; Gupta, V. K.; Kiefer, G. E. *Chem. Rev.* **1986**, *86*, 451–489.

(3) (a) Spencer, J.; Pfeffer, M. *Adv. Met.-Org. Chem.* **1998**, *6*, 103–144. (b) Dehand, J.; Pfeffer, M. *Coord. Chem. Rev.* **1976**, *18*, 327–352.

(4) (a) Beletskaya, I. P.; Cheprakov, A. V. *Chem. Rev.* **2000**, *100*, 3009–3066. (b) van der Boom, M. E.; Milstein, D. *Chem. Rev.* **2003**, *103*, 1759–1792. (c) Bedford, R. B.; Cazin, C. S. J.; Holder, D. *Coord. Chem. Rev.* **2004**, *248*, 2283–2321.

(5) Zhu, K.; Achord, P. D.; Zhang; Krogh-Jespersen, K.; Goldman, A. S. *J. Am. Chem. Soc.* **2004**, *126*, 13044–13053, and references cited therein.

(6) (a) Lowry, M. S.; Bernhard, S. *Chem. Eur. J.* **2006**, *12*, 7970–7977. (b) Termine, R.; Talarico, M.; Aiello, I.; Dattilo, D.; Pucci, D.; Ghedini, M.; Golemme, A. *Opto-Electron. Rev.* **2005**, *13*, 287–293. (c) Lai, S. W.; Che, C. M. *Top. Curr. Chem.* **2004**, *241*, 27–63. (d) Yam, V. W. W.; Wong, K. M. C.; Zhu, N. *J. Am. Chem. Soc.* **2002**, *124*, 6506–6507. (e) Zheng, G. Y.; Rillema, D. P. *Inorg. Chem.* **1998**, *37*, 1392–1397.

(7) (a) Albrecht, M.; van Koten, G *Angew. Chem., Int. Ed.* **2001**, *40*, 3750–3781. (b) Hissler, M.; Mc Garrah, J. E.; Connick, W. B.; Geiger, D. K.; Cummings, S. D.; Eisenberg, R. *Coord. Chem. Rev.* **2000**, *208*, 115–137, and references therein.

(8) (a) Mohr, F.; Privér, S. H.; Bhargava, S. K.; Bennett, M. A. *Coord. Chem. Rev.* **2006**, *250*, 1851–1888. (b) Thorn, D. L. *Organometallics* **1998**, *17*, 348–352. (c) Cheney, A. J.; Shaw, B. L. *J. Chem. Soc., Dalton Trans.* **1972**, 754–763.

(9) (a) Romeo, R.; Scolaro, L. M. *Perspect. Org. Chem. Synth.* **2003**, *287*, 208–221. (b) Romeo, R.; Plutino, M. R.; Scolaro, L. M.; Stoccoro, S.; Minghetti, G. *Inorg. Chem.* **2000**, *39*, 2712–2720. (c) Plutino, M. R.; Scolaro, L. M.; Romeo, R.; Grassi, A. *Inorg. Chem.* **2000**, *39*, 4749–4755.

(10) Dissociative substitution is rather common for complexes of the type *cis*-[Pt(C,C)(S,S)] (C = strong σ-donor carbon group; S = thioether, sulfoxide), no matter whether the carbon atom comes from an alkyl, an aryl, or a metalated aryl ligand. See: (a) Plutino, M. R.; Monsù Scolaro, L.; Romeo, R.; Grassi, A. *Inorg. Chem.* **2000**, *39*, 2712–2720. (b) Frey, U.; Helm, L.; Merbach, A. E.; Romeo, R. *J. Am. Chem. Soc.* **1989**, *111*, 8161–8165. (c) Alibrandi, G.; Minniti, D.; Monsù Scolaro, L.; Romeo, R. *Inorg. Chem.* **1989**, *28*, 1939–1943. (d) Alibrandi, G.; Bruno, G.; Lanza, S.; Minniti, D.; Romeo, R.; Tobe, M. L. *Inorg. Chem.* **1987**, *26*, 185–190. (e) Minniti, D.; Alibrandi, G.; Tobe, M. L.; Romeo, R. *Inorg. Chem.* **1987**, *26*, 3956–3958. (f) Lanza, S.; Minniti, D.; Moore, P.; Sachinidis, J.; Romeo, R.; Tobe, M. L. *Inorg. Chem.* **1984**, *23*, 4428–4833. (g) Lanza, S.; Minniti, D.; Romeo, R.; Moore, P.; Sachinidis, J.; Tobe, M. L. *J. Chem. Soc., Chem. Commun.* **1984**, 542–543. (h) Minniti, D. *J. Chem. Soc., Dalton Trans.* **1993**, 1343–1345.

10.1021/om701070f CCC: $40.75
Publication on Web 04/24/2008

Scheme 1. Reaction Pathway Proposed for the Cyclometalation of 1

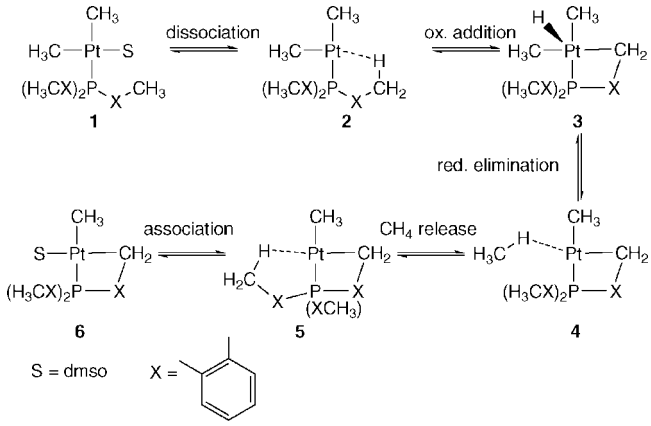

choosing among those complexes that have shown in other reactions, particularly nucleophilic substitutions, a pronounced propensity to dissociate ligands vacating a coordination site.[10] Thus, we proved that dissociation of a ligand is a preliminary step in the cycloplatination of the dinuclear platinum(II) compound of formula $[Pt_2(\mu\text{-}SEt_2)_2(Hbph)_4]$, ($Hbph^- = \eta^1$-biphenyl monoanion), yielding $[Pt_2(\mu\text{-}SEt_2)_2(bph)_2]$[11] and biphenyl, and of *cis*-$[Pt(Me)_2(dmso)(P(o\text{-}tol)_3)]$ (**1**), leading to the new C,P-cyclometalated compound $[Pt\{CH_2C_6H_4P(o\text{-}tolyl)_2\text{-}\kappa C,P\}(Me)(dmso)]$ (**6**) with liberation of methane.[12] On the basis of spectrophotometric and ^1H NMR kinetic studies, cyclometalation of **1** has been proposed to develop along a multistep mechanism consisting of (i) reversible dissociation of the dmso ligand to give the coordinatively unsaturated 14-electron T-shaped intermediate $[Pt(Me)_2(P(o\text{-}tol)_3)]$ (**2**), (ii) intramolecular oxidative addition of the C−H bond of a methyl group on the $P(o\text{-}tol)_3$ ligand to give the pentacordinate cyclometalated hydride species **3**, (iii) reductive elimination of methane to give the σ-complex **4**, which evolves to the unsaturated 14-electron species **5**, and (iv) fast reassociation of a dmso ligand to give the final C,P-cyclometalated square-planar product **6** (see Scheme 1). Cyclometalation in the 3-coordinate 14-electron T-shaped intermediate **2** has been suggested to be initiated by an agostic interaction of the unsatured Pt center with the C−H bond of a methyl group on the $P(o\text{-}tol)_3$ ligand. Neither fairly high steric congestion brought about by the P(o-tolyl)$_3$ ligand (cone angle 198°, from crystallographic measurements)[13] nor the favorable formation of a five-membered C−M−P ring were sufficient to promote cycloplatination directly from the 16-electron species **1**, as observed, for example, in platinum derivatives containing the "$Pt\{CH_2C_6H_4P(o\text{-}tolyl)_2\text{-}\kappa C,P\}$" molecular fragment.[14]

In addition to confirming the reaction model and a rare dissociative reaction pathway, inferred from the kinetic analysis, density functional calculations allow for a measure of the energies and a better understanding of the bonding and structural features of the species intercepted along the potential energy surface (PES) of the reaction. In spite of the large size of this complex, the calculations have been performed on the real system.

Chart 1. Possible Conformations for Complex 1

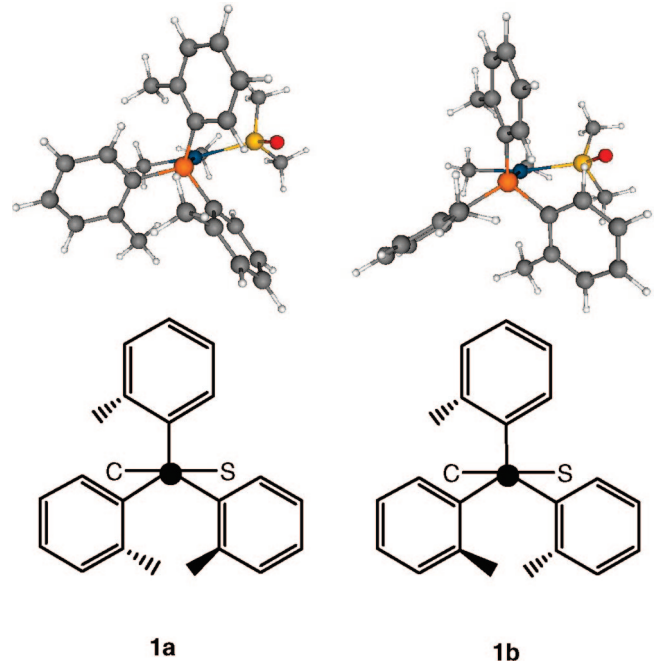

Results and Discussion

Structural Properties. Geometry optimizations were performed for the initial and the final cyclometalated complexes and for the main intermediates, and the calculated geometries are shown in Figure 1. According to low- and room-temperature ^1H and ^{31}P NMR spectra, complex **1** exists in two differently populated conformations, **1a**,**b**, present in a ca. 4:1 ratio.[15] The relative conformations of **1a**,**b** were assigned through NMR spectroscopy from the connectivities in 2D-COSY and NOE cross peaks in 2D-NOESY experiments. The results were fully consistent with restricted rotation around the $P-C_{ipso}$ aryl bonds, while the M−P rotation remains rapid. When the temperature was increased, the ^1H NMR spectra of **1a**,**b** maintained their "static" pattern to the onset of easy and fast ortho platination leading to $[Pt\{CH_2C_6H_4P(o\text{-}tolyl)_2\text{-}\kappa C,P\}(Me)(dmso)]$ (**6**), a new C,P-cyclometalated compound of Pt(II), and liberating methane. Generally, for simpler PPh_3 complexes, the process of highest energy is M−P rotation, with only few cases being reported in which restricted P−C rotation is evidenced at very low temperature.[16] For $P(o\text{-}tolyl)_3$ complexes restricted $P-C_{ipso}$ aryl rotation occasionally becomes higher in energy than M−P

(11) Plutino, M. R.; Monsù Scolaro, L.; Albinati, A.; Romeo, R. *J. Am. Chem. Soc.* **2004**, *126*, 6470–6484.

(12) Romeo, R.; Plutino, M. R.; Romeo, A. *Helv. Chim. Acta* **2005**, *88*, 507–522.

(13) Ferguson, G.; Roberts, P. J.; Alyea, E. C.; Khan, M. *Inorg. Chem.* **1978**, *17*, 2965–2967.

(14) (a) Fornies, J.; Martin, A.; Navarro, R.; Sicilia, V.; Villarroya, P. *Organometallics* **1996**, *15*, 1826–1833. (b) Casas, J. M.; Fornies, J.; Fuertes, S.; Martìn, A.; Sicilia, V. *Organometallics* **2007**, *26*, 1674–1685, and references therein. (c) Chappell, S. D.; Cole-Hamilton, D. J. J. *Chem. Soc. Dalton Trans.* **1983**, 1051–1057.

(15) Particularly helpful resonances for the NMR analysis in $CDCl_3$ were (i) a $^{31}P\{^1H\}$ singlet flanked by platinum satellites (at δ 28.3, $^1J(Pt,P) =$ 1824 Hz for **1a** and at δ 27.1, $^1J(Pt,P) =$ 1881 Hz for **1b**), (ii) two sets of three different singlet signals for the methyl substituent groups in positions ortho to the aryl rings in the phosphane ligand (δ 2.84, 1.83, and 1.55 for **1a** and δ 3.00, 2.05, and 1.53 for **1b**), and (iii) two sets of signals for the methyl protons of the dimethyl sulfoxide ligand (δ 2.94, $^3J(Pt,H) =$ 13.9, 2.20 Hz, $^3J(Pt,H) =$ 13.1 Hz for **1a**; δ 3.06, $^3J(Pt,H) =$ 15.6 and 2.88 Hz, $^3J(Pt,H) =$ 16.0 hz for **1b**).

(16) (a) Davies, S. G.; Derome, A. E.; McNally, J. P. *J. Am. Chem. Soc.* **1991**, *113*, 2854–2861. For reviews, see: (b) Mislow, K. *Acc. Chem. Res.* **1976**, *9*, 26–33. (c) Mislow, K. *Pure Appl. Chem.* **1971**, *225*, 549–562. (d) Mislow, K.; Gust, D.; Finocchiaro, P.; Boettcher, R. J. *Top. Curr. Chem.* **1974**, *47*, 1–28. (e) Fanizzi, F. P.; Lanfranchi, M.; Natile, G.; Tiripicchio, A. *Inorg. Chem.* **1994**, *33*, 3331–3339.

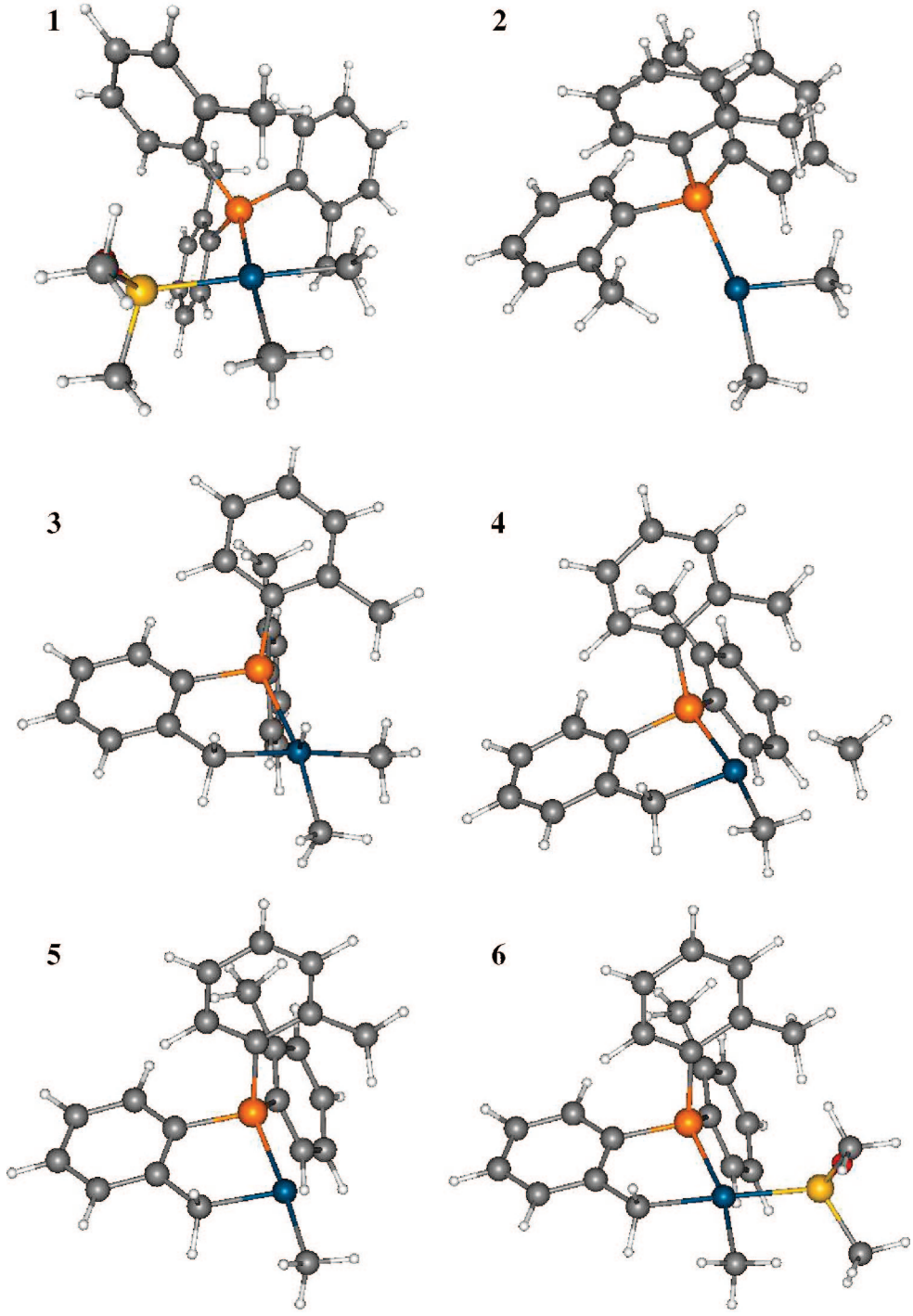

Figure 1. DFT optimized geometries of complexes **1**−**6**.

rotation. For instance, line-shape analysis of the proton *o*-methyl resonances gave a $\Delta G^{\ddagger}_{238}$ value of of 50.2 kJ mol^{-1} for ring exchange in $[Cr(C_6H_6)(CO)_2P(o\text{-tolyl})_3]$,[17] considerably higher than for analogous processes in $[Cr(CO)_5(P(o\text{-tolyl})_3)]$ and $[Fe(CO)_4(P(o\text{-tolyl})_3)]$ ($\Delta G^{\ddagger} = 38.6$ and 44.6 kJ mol^{-1}, respectively).[18] Unexpectedly, the two atropisomers **1a**,**b** appear quite inert and the expected collapse of the *o*-tolyl subspectrum at room temperature is not observed. Our calculations show two minima in the potential energy surface of **1**, whose geometries correspond to the proposed structures **1a**,**b** in Chart 1, the former being slightly more stable (7 kJ mol^{-1}) and considered hereafter as **1**.

As can be seen from Figure 1, the DFT optimization confirms that the 3-coordinate 14-electron intermediate **2** has a T-shaped configuration and is stabilized by a classical $Pt\cdots\eta^2$-*HC* agostic mode between the unsaturated metal and the methyl group of a dangling *o*-tolyl ring. The main geometrical features that define the stereochemistry of the agostic bond are (i) the elongation of the C(1)−H(1) bond length (1.13 Å) relative to the geminal nonagostic C(1)−H(2)(3) bond lengths (1.10 Å) which point away from the metal, (ii) the close proximity of

(17) Howell, J. A. S.; Palin, M. G.; McArdle, P.; Cunningham, D.; Goldschmidt, Z.; Gottlieb, H. E.; Hezroni-Langerman, D. *Organometallics* **1993**, *12*, 1694–1701.

(18) Howell, J. A. S.; Palin, M. G.; McArdle, P.; Cunningham, D.; Goldschmidt, Z.; Gottlieb, H. E.; Hezroni-Langerman, D. *Inorg. Chem.* **1991**, *30*, 4685–4687.

the C(1)−H(1) bond to the vacant coordination site and to the metal, revealed by the Pt−H(1) and Pt−C(1) distances of 2.04 and 2.88 Å, respectively, and (iii) the limited rotation of the methyl group, around the C(2)−C(1) bond, as inferred from the Pt−P−C(1)−H(1) torsion angle (14°). All these data fit well with the distinction made by Mealli et al.[19] between classical and nonclassical metal···H_3C−C interactions as a result of a close examination of the structural properties of a large amount of "agostic" compounds. A survey of the X-ray data on a few isolated 3-coordinate 14e d^8-ML_3 species shows C−H bonds involved in agostic interactions to the empty coordination site of otherwise T-shaped d^8 complexes. These examples include the cationic $[Pt(R)(P-P)]^+$ complexes (P−P = chelating ligand, R = ethyl, norbornyl),[20] the very recent $[Pt(CH_3)(^iPr_3P)_2]^+$,[21] and the novel "T-shaped 14-electron" platinum(II) cations *trans*-$[Pt(CH_3)L_2]^+$ (L = $PR_2(2,6\text{-}Me_2C_6H_3)$, R = Ph, Cy).[22] Related complexes of isoelectronic Ni(II),[23] Rh(I),[24] and Pd(II)[25] have also been described. A combined kinetic and DFT study of the uncatalyzed isomerization of cationic solvent complexes of the type *cis*-$[Pt(R')(S)(PR_3)_2]^+$ (R′ = linear and branched alkyls or aryls, S = solvent) to their trans isomers has defined as the *β-hydrogen kinetic effect* the great acceleration of the reaction rate resulting from the stabilization of the TS and of the "cis-like" three-coordinate $[Pt(R')(PR_3)_2]^+$ intermediates through an incipient agostic interaction whose energy was estimated by both kinetic and computational data to be in the range of 21–33 kJ mol^{-1}.[26] The energy barrier for the conversion of the "cis-like" into a geometrically distinct "trans-like" T-shaped 14-electron 3-coordinate species was found to be very low (∼8–21 kJ mol^{-1}). The differences between the "agostic" 14-electron T-shaped intermediates $[Pt(Me)_2(P(o\text{-}tol)_3)]$ and $[Pt(Et)(PR_3)_2]^+$ appear to be considerable, as far the charge (neutral vs cationic), the agostic connectivity (δ vs β), and the fluxionality are concerned. Thus, the unsaturated species **2** does not undergo any fluxional geometrical conversion but the incipient interaction of the metal with the hydrogen eventually results in an intramolecular C−H activation leading to a C,P-cyclometalated pseudo-square-pyramidal pentacoordinate species, **3**, with the hydrogen ligand in the apical position (see Figure 1).

Table 1. Reaction Enthalpies and Free Energies (Values in kJ mol^{-1}) and Reaction Entropies (Values in J mol^{-1} K^{-1}) for Each Step of the Cyclometalation of 1

reacn	ΔH_{gas}	ΔS_{gas}	ΔG_{gas}	ΔH_{sol}	ΔG_{sol}
1 → **2**	85	179	32	76	23
2 → **3**	78	20	72	79	73
3 → **4**	−105	−28	−97	−107	−99
4 → **5**	9	184	−46	12	−43
5 → **6**	−95	−198	−36	−88	−29
1 → **6** (total)	−28	157	−75	−28	−75

Several theoretical studies have indicated that these reaction intermediates should have square-pyramidal geometry,[27] but only recently have two papers appeared describing the isolation and structural characterization of such compounds.[28] In compound **3** the hydride occupies the apical position. Structural parameters relative to the five-membered metallacycle are similar to those observed in other complexes containing it.[14] The phosphorus atom exhibits a tetrahedral arrangement, with the two aryl groups projecting with different orientations on opposite sides of the square base. A slight tilt away from the square coordination plane is also observed for the aryl fragment of the cyclometalated ring. Reductive elimination of **3** results in the σ complex **4**, which consists essentially of a T-shaped three-coordinate species with a molecule of methane close to the vacant coordination site (Pt−C separation 2.78 Å). Although their existence is supported only by a small amount of indirect experimental evidence, such as time-resolved infrared spectroscopy at the nanosecond scale,[29] σ complexes have been identified as metastable minima in several theoretical investigations of C−H bond activation.[27]

Two different isomers are possible for the three-coordinate T-shaped species **5**, resulting from reductive elimination of **3** and methane liberation, according to the position of the residual methyl ligand in a position cis or trans to the phosphane group: **5a**,**b**, respectively. The trans isomer **5b** has been found to be more stable by 26 kJ mol^{-1} due to (i) a trans destabilization of the methyl ligand that is smaller with a phosphane than with the methylphenyl ligand and (ii) the stabilization by an agostic metal···H_3C−C interaction involving a methyl group from a second *o*-tolyl ring on the cyclometalated phosphine. Such an interaction is not permitted in **5a**, since the unsatured coordination site lies far away (in a trans position) from the coordinated phosphorus atom. The agostic interaction is disrupted by the reassociation of a dmso ligand to give the final stable square-planar cyclometalation product **6** (see Figure 1). In this latter compound the cyclometalated ring lies almost coplanar to the coordination plane and *o*-tolyl rotation around the P−C_{ipso} bond is very fast, at room temperature, as inferred from the single resonances observed for the two residual *o*-tolyl rings and for the protons of the methylene group.[12]

Energy Profiles. The energies calculated for compounds **1**−**6** (see Table 1) and the subsequent frequency analysis allowed us to build the enthalpy and free energy diagrams reported in Schemes 2 and 3. Since the values in the gas phase and in solution are very close (within 2–9 kJ mol^{-1}), as expected on the basis of the low polarity of the considered solvent, only the values in solution have been reported and discussed. The

(19) Baratta, W. M.; Mealli, C.; Herdtweck, E.; Ienco, A.; Mason, S. A.; Rigo, P. *J. Am. Chem. Soc.* **2004**, *126*, 5549–5562.
(20) (a) Carr, N.; Mole, L.; Orpen, A. G.; Spencer, J. L. *J. Chem. Soc., Dalton Trans.* **1992**, 2653–2662. (b) Mole, L.; Spencer, J. L.; Carr, N.; Orpen, A. G. *Organometallics* **1991**, *10*, 49–52.
(21) Ingleson, M. J.; Mahon, M. F.; Weller, A. S. *Chem. Commun.* **2004**, 2398–2399.
(22) Baratta, W.; Stoccoro, S.; Doppiu, A.; Herdtweck, E.; Zucca, A.; Rigo, P. *Angew. Chem., Int. Ed.* **2003**, *42*, 105–109.
(23) Hay-Motherwell, R.; Wilkinson, G.; Sweet, T. K. N.; Hursthouse, M. B. *Polyhedron* **1996**, *15*, 3163–3166.
(24) (a) Yared, Y. W.; Miles, S. L.; Bau, R.; Reed, C. A. *J. Am. Chem. Soc.* **1977**, *99*, 7076–7078. (b) Urtel, H.; Meier, C.; Eisenträger, F.; Rominger, F.; Joschek, J. P.; Hofmann, P. *Angew. Chem., Int. Ed. Engl.* **2001**, *40*, 781–784.
(25) (a) Stambuli, J. P.; Bühl, M.; Hartwig, J. F. *J. Am. Chem. Soc.* **2002**, *124*, 9346–9347. (b) Yamashita, M.; Hartwig, J. F. *J. Am. Chem. Soc.* **2004**, *126*, 5344–5345. (c) Stambuli, J. P.; Incarvito, C. D.; Bühl, M.; Hartwig, J. F. *J. Am. Chem. Soc.* **2004**, *126*, 1184–1194. (d) Campora, J.; Gutiérrez-Puebla, E.; Lopez, J. A.; Monge, A.; Palma, P.; Del Rio, D.; Carmona, E. *Angew. Chem., Int. Ed.* **2001**, *40*, 3641–3644.
(26) Romeo, R.; D'Amico, G.; Sicilia, E.; Russo, N.; Rizzato, S. *J. Am. Chem. Soc.* **2007**, *129*, 5744–5755.
(27) (a) Hill, G. S.; Puddephatt, R. J. *Organometallics* **1998**, *17*, 1478–1486. (b) Siegbahn, P. E. M.; Crabtree, R. H. *J. Am. Chem. Soc.* **1996**, *118*, 4442–4450. (c) Bartlett, K. L.; Goldberg, K. I.; Borden, W. T. *J. Am. Chem. Soc.* **2000**, *122*, 1456–1465. (d) Bartlett, K. L.; Goldberg, K. I.; Borden, W. T. *Organometallics* **2001**, *20*, 2669–2678. (e) Heiberg, H.; Johansson, L.; Gropen, O.; Ryan, O. B.; Swang, O.; Tilset, M. *J. Am. Chem. Soc.* **2000**, *122*, 10831–10845. (f) Gilbert, T. M.; Hristov, I.; Ziegler, T. *Organometallics* **2001**, *20*, 1183–1189.
(28) (a) Fekl, U.; Kaminsky, W.; Goldberg, K. I. *J. Am. Chem. Soc.* **2001**, *123*, 6423–6424. (b) Reinartz, S.; White, P. S.; Brookhart, M.; Templeton, J. L. *J. Am. Chem. Soc.* **2001**, *123*, 6425–6426.
(29) (a) Lian, T.; Bromberg, S. E.; Yang, H.; Proulz, G.; Bergman, R. G.; Harris, C. B. *J. Am. Chem. Soc.* **1996**, *118*, 3769–3770. (b) Bromberg, S. E.; Yang, H.; Asplund, M. C.; Lian, T.; McNamara, B. K.; Kotz, K. T.; Yeston, J. S.; Wilkens, M.; Frei, H.; Bergman, R. G.; Harris, C. B. *Science* **1997**, *278*, 260–263.

Scheme 2. Enthalpy Diagram for the Whole Cyclometalation Reaction of 1 in Chloroform Solution

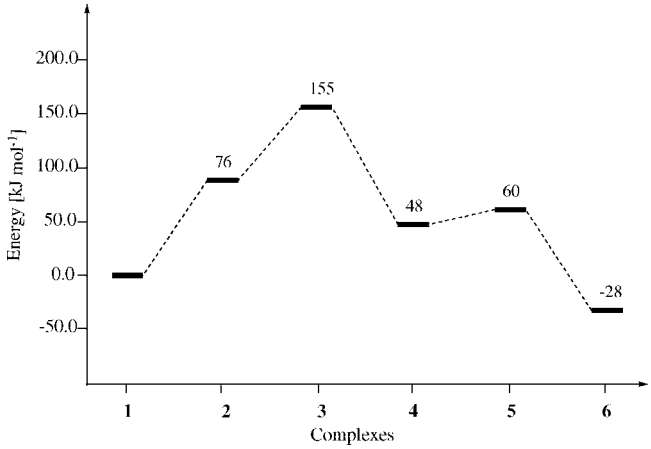

Scheme 3. Free Energy Diagram for the Whole Cyclometalation Reaction of 1 in Chloroform Solution

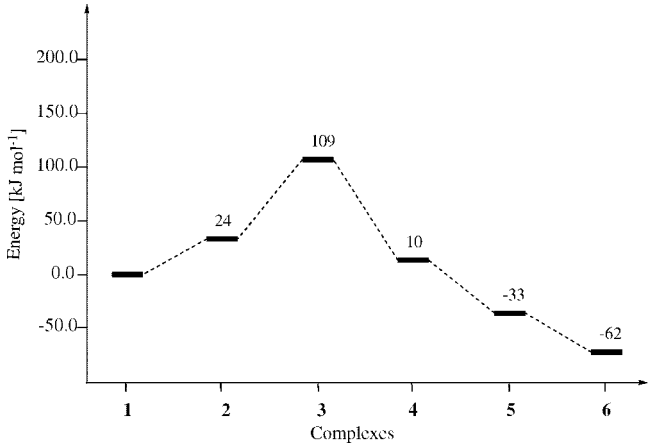

enthalpy diagram in Scheme 2 shows that the first two steps are endothermic, by 76 kJ mol^{-1} for the dmso dissociation and by 79 kJ mol^{-1} for the oxidative addition, while two of the last three steps are exothermic, by 107 kJ mol^{-1} for the methane reductive elimination and 88 kJ mol^{-1} for the dmso reassociation. In contrast, the loss of methane from **4** is slightly endothermic, by 12 kJ mol^{-1}, leading to an overall favorable reaction enthalpy of -28 kJ mol^{-1}. Scheme 3 shows that the free energy variations for the oxidative addition and reductive elimination are very close to the corresponding enthalpy variations (within 6–8 kJ mol^{-1}), while those of the dmso dissociation, methane loss, and reassociation are quite different (by ca. 50 kJ mol^{-1}), due to the high translational entropy contribution associated with these processes. The translational entropy contribution affects also the methane dissociation from **4**, whose free energy becomes slightly negative, by 43 kJ mol^{-1}.

C−H Bond Activation. Since the dmso dissociation step is a barrierless ligand dissociation process, its activation enthalpy coincides with the corresponding reaction enthalpy, for which a value of 76 kJ mol^{-1} has been calculated (see Table 1). This value is in good agreement with the experimental value of 81 $\pm$ 2 kJ mol^{-1} estimated from a combined spectrophotometric and variable-temperature ^{1}H NMR kinetic study of ligand dissociation in $CDCl_3$.[12] Moreover, the reaction free energy of 24 kJ mol^{-1} calculated for the dmso dissociation compares well with the value 24.2 $\pm$ 0.1 kJ mol^{-1} for the reaction free energy, deduced through the equation $\Delta G^\circ = -RT \ln K$ (the value of the experimental equilibrium constant $K = (5.7 \pm 0.1) \times 10^{-5}$ for this step was estimated from kinetic data).[12]

We then searched for the transition state of the oxidative addition step, the dmso dissociation and association steps being clearly barrierless. Unexpectedly, in spite of several efforts, no transition state could be found for this process. The absence of a clear transition state for the oxidative addition from **2** to **3** is supported by the difficulties found in the geometry optimization of the pentacoordinate product **3**, which collapses easily to **2** when starting from geometries slightly different from the calculated minimum. In particular, no isomer with the hydride ligand in the basal plane could be optimized for this reason. To confirm this point, a linear transit calculation has been performed for the oxidative addition from **2** to **3**, using as the reaction coordinate the C−H distance which has been increased from 1.09 Å, the value calculated in **2** which corresponds to a C−H bond, to 2.61 Å, the value calculated in **3** which corresponds to the distance between the coordinating C atom of the methylphenyl group and the hydride ligand, resulting after complete C−H breaking. The result is shown in Figure SI1 in the Supporting Information and indicates an almost monotonic increase of the energy with a barely noticeable maximum at a Pt−C value of 2.05 Å, corresponding to a structure very close to that optimized for the oxidative addition product **3** and an energy of only 6 kJ mol^{-1} above it; since a maximum in this linear transit curve is an upper limit for the transition state energy, this result would support that the oxidation reaction of **2** is barrierless. However, since the transition-state search algorithm of the ADF package employed in all the calculations is not very efficient, we further investigated this point by performing geometry optimization on **2** and **3** and a transition state search at essentially the same level of theory using the Jaguar package (see Computational Details). The reaction energy, enthalpy, and free energy calculated with Jaguar are very close to those calculated with ADF (see Table SI2 in the Supporting Information). Moreover, employing the QST algorithm included in this package, we could find a transition state with only one imaginary frequency of 280 cm^{-1}, whose associated eigenvectors correspond to the expected reaction coordinate. The energy of this transition state is only 1 kJ mol^{-1} above that of **3**, and the introduction of ZPE, thermal, entropic, and solvation contributions lowers its enthalpy and free energy even below (by 4–8 kJ mol^{-1}) those of **3**. An energy evaluation with the ADF program on the Jaguar optimized transition state confirms this result, leading for this structure to essentially the same energy as that of **3** and slightly lower enthalpy and free energy. Therefore, we can reasonably conclude that the oxidation reaction of **2** is barrierless or has an extremely late transition state, barely distinguishable from the product **3**, so that the activation enthalpy for this step can be assumed to coincide with its reaction enthalpy of $+79$ kJ mol^{-1}. This value is in good agreement with the experimental value of 82 $\pm$ 4 kJ mol^{-1} estimated from the variable-temperature ^{1}H NMR kinetic studies in $CDCl_3$.[12]

Inertness of the Four-Coordinate complex 1 to C−H Activation. In order to confirm the experimental evidence that the square-planar 16-electron platinum complex **1** is kinetically inert toward cyclometalation and that the latter process requires the preliminary dmso dissociation with formation of the 3-coordinate 14-electron species **2**, we calculated the energy profile for the intramolecular C−H oxidative addition of a methyl group of the P(*o*-tol)$_3$ ligand directly on **1** and compared it with that for the same oxidative addition from the 14-electron species **2** (see above). For both the **1** to **3** and **2** to **3** processes

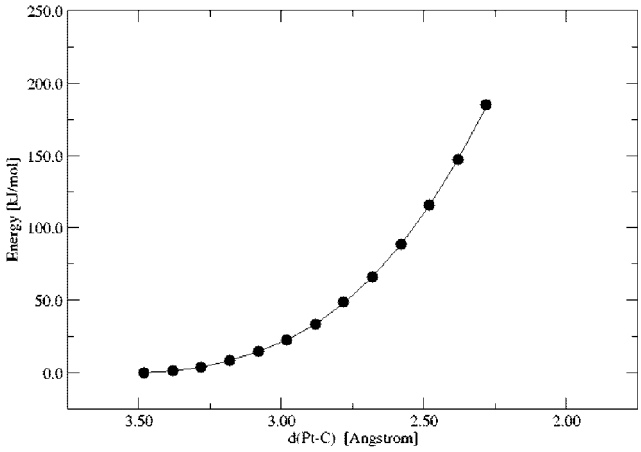

Figure 2. Energy profile for the direct **1** to **3** oxidative addition.

we first performed a linear transit calculation, using as reaction coordinate the Pt−C distance which has been decreased from, respectively, 3.48 Å, the value calculated in **1**, or 2.88 Å, the value calculated in **2** and corresponding to an agostic interaction, to 2.18 Å, the value calculated for the Pt−C bond in **3**. The linear transit for the **2** to **3** oxidative addition shows the same features observed using as reaction coordinate the C−H bond (see Figure SI1 in the Supporting Information), with an almost monotonic increase of the energy and a barely distinguishable maximum for a geometry very close to that of the oxidative addition product **3**. In contrast, the linear transit for the **1** to **3** oxidative addition in Figure 2, after an initial plateau, shows a very steep monotonic increase of the energy, reaching for the final Pt−C value of 2.18 Å an energy of ca. 150 kJ mol^{-1}, well above that of the oxidative addition product **3**, indicating that the Pt−C bond is not a good reaction coordinate and that the approach of the C−H bond does not assist the dmso dissociation. This is a further confirmation that the underpinnings of easy ligand dissociation in electron-rich complexes having a set of donor atoms of the type *cis*-[Pt(C,C)(S,S)] or *cis*-[Pt(C,C)(P,S)] (C = strong σ-donor carbon group; P = phosphane; S = thioether, sulfoxide) are only electronic in nature.[10] Thus, for the oxidative addition of **1** to **3**, the minimum energy path along the potential energy surface (PES) passes though a preliminary dissociation of the dmso ligand (leading to **2**), while the channel corresponding to a direct approach of the *o*-methyl group in **1** to the platinum atom, although initially lower in energy, leads later to a very steep valley without any low-energy path to **3**. Further insight into the detailed path for the intramolecular C−H oxidative addition of a methyl group of the P(*o*-tol)$_3$ ligand on **1** can be gained by the three-dimensional section of the PES along the Pt−C(methyl) and Pt−S(dmso) distances, for which a schematic overview of the 2D contour plots is reported in Figure 3. Complexes **1**−**3** appear as minima on this surface, **2** being slightly lower in energy than the asymptotic channel corresponding to the dmso detatchment from **1**, due to the formation of the agostic interaction. In Figure 4 are reported the energy profiles along the approximate **1** → **3** reaction coordinates built by (i) first lengthening the Pt−S distance until dmso dissociation and then decreasing the Pt−C distance (profile a) or (ii) directly decreasing the Pt−C distance (profile b); the figure shows that the former coordinate is a good approximation to the minimum energy path for oxidative addition (corresponding to the **1** → **2** → **3** mechanism), while the latter coordinate does not correspond to any low-energy reactive channel.

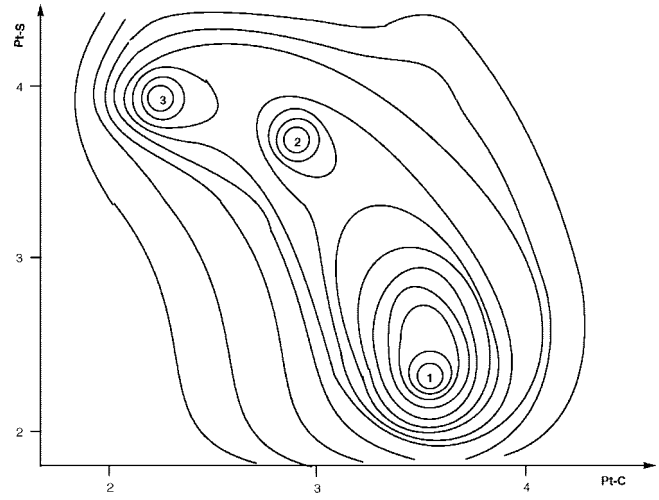

Figure 3. 2D contour plot of the PES section, for the oxidative addition of **1** to **3**, along the Pt−S and Pt−C bond lengths.

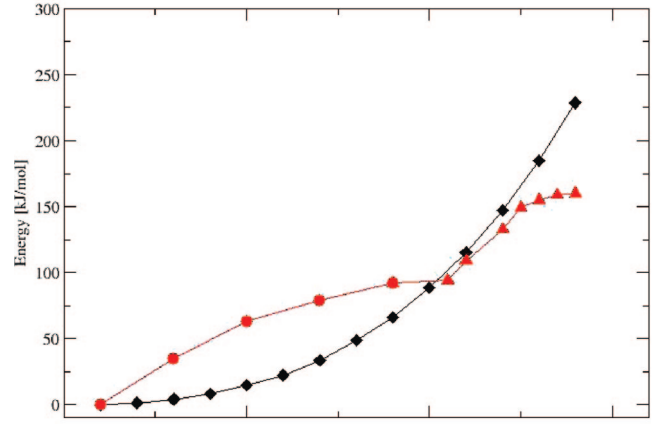

Figure 4. Energy profiles along the approximate **1** → **3** reaction coordinates built by (a) first lengthening the Pt−S distance until dmso dissociation and then decreasing the Pt−C distance (red ● and red ▲) or (b) directly decreasing the Pt−C distance (◆).

Reductive Elimination. We mentioned before that hydrido-platinum(IV) complexes are firmly established both as stable compounds and as short-lived reaction intermediates, particularly in platinum-catalyzed selective alkane functionalization reactions, and can be generated by protonation of 16-electron square-planar platinum(II)[30] or, as in the present case, by concerted oxidative addition of C−H bonds to 14-electron T-shaped platinum(II) precursors.[31] Since it is extremely difficult to obtain direct mechanistic information on the initial steps of alkane activation via oxidative addition, the study of alkane reductive

(30) (a) Puddephatt, R. J. *Coord. Chem. Rev.* **2001**, *219–221*, 157–185. (b) De Felice, V.; De Renzi, A.; Panunzi, A.; Tesauro, D. *J. Organomet. Chem.* **1995**, *488*, C13–C14. (c) Hill, G. S.; Rendina, L. M.; Puddephatt, R. J. *Organometallics* **1995**, *14*, 4966–4968. (d) Stahl, S. S.; Labinger, J. A.; Bercaw, J. E. *J. Am. Chem. Soc.* **1995**, *117*, 9371–9372. (e) Stahl, S. S.; Labinger, J. A.; Bercaw, J. E. *J. Am. Chem. Soc.* **1996**, *118*, 5961–5976. (f) O'Reilly, S. A.; White, P. S.; Templeton, J. L. *J. Am. Chem. Soc.* **1996**, *118*, 5684–5689. (g) Hill, G. S.; Puddephatt, R. J. *J. Am. Chem. Soc* **1996**, *118*, 8745–8746. (h) Reinartz, S.; White, P. S.; Brookhart, M.; Templeton, J. L. *Organometallics* **2000**, *19*, 3854–3866. (i) Canty, A. J.; Fritsche, S. D.; Jin, H.; Patel, J.; Skelton, B. W.; White, A. H. *Organometallics* **1997**, *16*, 2175–2182. (j) Prokopchuk, E. M.; Jenkins, H. A.; Puddephatt, R. J. *Organometallics* **1999**, *18*, 2861–2866. (k) Prokopchuck, E. M.; Puddephatt, R. J. *Organometallics* **2003**, *22*, 787–796.

(31) (a) Wick, D. D.; Goldberg, K. I. *J. Am. Chem. Soc.* **1997**, *119*, 10235–10236. (b) Lersch, M.; Tilset, M. *Chem. Rev.* **2005**, *105*, 2471–2526, and references therein.

elimination, the microscopic reverse process which passes through the same transition states, enables for a better understanding of the C−H activation mechanism. As for the oxidative addition, in spite of several attempts, we did not find any transition state for the reductive elimination process. To confirm the absence of a transition state, a linear transit calculation has also been performed for the methane reductive elimination step from **3** to **4**. We used again as reaction coordinate the C−H distance between the leaving hydride and methyl ligands, which has been decreased from 2.60 Å, the value calculated in **3**, to 1.09 Å, the value calculated for the C−H bond in the eliminated methane molecule. The result is shown in Figure SI2 in the Supporting Information and indicates, again, an almost monotonic decrease of the energy with a barely noticeable maximum at a Pt−C value of 2.55 Å, corresponding to a structure very close to that optimized for the reactant **3** and an energy of only 5 kJ mol^{-1} above it. As for the oxidative addition, we further investigated the **3** → **4** reductive elimination step by performing a geometry optimization on **3** and **4** and a transition state search using the Jaguar package (see above). We calculated a reaction energy, enthalpy, and free energy very close to those calculated with ADF (see Table SI2 in the Supporting Information) and found a transition state with only one imaginary frequence of 217 cm^{-1} corresponding to the expected reaction coordinate. The energy of this transition state is only 2 kJ mol^{-1} above **3**, and the introduction of ZPE, thermal, entropic, and solvation contributions lowers its enthalpy and free energy even below (by 6–9 kJ mol^{-1}) those of **3.** An energy evaluation with the ADF program on the Jaguar optimized transition state confirms this result, giving for this structure an energy 1 kJ mol^{-1} below **3** and slightly lower enthalpy and free energy. Therefore, for the same reasons discussed above, we can reasonably state that the methane reductive elimination from **3** is barrierless or has an extremely early transition state, barely distinguishable from **3** itself, and thus this step can be assumed to occur without any energy barrier. The lack of an energy barrier for the reductive eliminations from **3** to **2** (the inverse reaction of the **2** to **3** oxidative addition step) and from **3** to **4** is in agreement with literature data. For instance, recent B3LYP calculations on the reductive elimination of methane from the five-coordinate model complexes *cis*-$[PtMe_2HL_2]^+$ (L = NH_3, PH_3) and on the microscopic reverse oxidative additions have shown that[27a] (i) the five-coordinate Pt(IV) species prefer a square-pyramidal geometry, (ii) the concerted reductive elimination reactions leading to the σ methane complex *cis*-$[PtMe(CH_4)L_2]^+$ are characterized by very low activation energies, and (iii) the reverse methane activation reaction was found to be easier with L = NH_3 than with L = PH_3. Although the role of hydridoplatinum(IV) intermediates appears to be well-established in the activation of alkanes or arenes[29,32] and in the protonolysis of alkyl− or aryl−platinum(II) bonds,[28] and we did characterize a hydridoplatinum(IV) species in our calculations, the lack of well-defined energy barriers along the potential energy surface is a further reminder of the difficulty in distinguishing the proposed reaction pathway via oxidative addition from alternative pathways such as the metathesis mechanism for C−H bond activation or concerted proton attack at the Pt−C bond (classical S_E2 mechanism).[33]

Conclusions

The ^1H NMR and kinetic work that has preceded this theoretical study has provided clear-cut experimental evidence that the molecule of *cis*-$[Pt(Me)_2(dmso)(P(o\text{-}tol)_3)]$ exists in $CDCl_3$ solution in two differently populated conformations (in the ratio **1a**:**1b** ≅ 4), which maintain their "static" pattern to the onset of easy and fast ortho platination, leading to $[Pt\{CH_2C_6H_4P(o\text{-}tolyl)_2\text{-}\kappa C,P\}(Me)(dmso)]$ (**6**), a new C,P-cyclometalated compound of Pt(II), and liberating methane. A prerequisite for C−H bond activation at the methyl group of the *o*-tolyl ring is dissociation of the coordinated dmso molecule and the formation of a reactive *cis*-$[Pt(Me)_2(P(o\text{-}tol)_3)]$ 3-coordinate 14-electron species. Dissociation of dmso was found to be relatively fast with respect to the rate of C−H bond activation, suggesting an initial pre-equilibrium and subsequent rate-determining oxidative addition−reductive elimination sequential steps leading to the final cyclometalated compound. The results of this DFT analysis support fully the reaction pathway inferred from the kinetics and document the involvement of one 5-coordinate Pt(IV) complex, two 3-coordinate Pt(II) species, and a Pt(II) C−H σ complex as reaction intermediates. Intramolecular C−H activation at the starting 16-electron complex was found to be energetically unfavorable. Thus, it is possible to conclude that, at least in this case, 3-coordinate intermediates are *necessarily* intermediates in C−H bond activation.[34] The principle of microscopic reversibility requires also that a ligand must be lost from the square-planar Pt(II) complex **6** prior to methane oxidative addition, a fundamental step in Shilov alkane oxidation system.[1] The structural analysis of the transient species involved in the mechanistic model reveals that both 3-coordinate Pt(II) 14-electron species have a T-shaped conformation and are stabilized by agostic hydrogen interactions with the metal at the vacant coordination site. A remarkable feature is that the collapse of the 5-coordinate species **3** to **4**, in the reductive elimination step, involves a selective Pt−C bond breaking at the methyl group in a position trans to the strong σ-donor carbon atom of the methylene group of the chelated ring, thus giving the opportunity for the resulting T-shaped three-coordinate isomer to be stabilized through hydrogen agostic interactions. Reductive eliminations from **3** to **2** and from **3** to **4** are barrierless processes.

Computational Details

DFT calculations were performed using the Amsterdam Density Functional (ADF2000.02) program developed by Baerends et al.[35] We used the local VWN exchange-correlation potential[36] with Becke's nonlocal exchange correction[37] and Perdew's correlation correction (BP86).[38] Relativistic corrections were introduced by

(32) (a) Williams, T. J.; Labinger, J. A.; Bercaw, J. E. *Organometallics* **2007**, *26*, 281–287. (b) Driver, T. G.; Williams, T. J.; Labinger, J. A.; Bercaw, J. E. *Organometallics* **2007**, *26*, 294–301. (c) Zhong, H. A.; Labinger, J. A.; Bercaw, J. E. *J. Am. Chem. Soc.* **2002**, *124*, 1378–1399. (d) Johansson, L.; Tilset, M.; Labinger, J. A.; Bercaw, J. E. *J. Am. Chem. Soc.* **2000**, *122*, 10846–10855. (e) Procelewska, J.; Zahl, A.; van Eldik, R.; Zhong, H. A.; Labinger, J. A.; Bercaw, J. E. *Inorg. Chem.* **2002**, *41*, 2808–2810. (f) Johansson, L.; Ryan, O. B.; Tilset, M. *J. Am. Chem. Soc.* **1999**, *121*, 1974–1975. (g) Johansson, L.; Ryan, O. B.; Römming, C.; Tilset, M. *J. Am. Chem. Soc.* **2001**, *123*, 6579–6590. (h) Periana, R. A.; Taube, D. J.; Gamble, S.; Taube, H.; Satoh, T.; Fujii, H. *Science* **1998**, *280*, 560–564. (i) Fekl, U.; Goldberg, K. I. *Adv. Inorg. Chem.* **2003**, *54*, 259–320.

(33) Romeo, R.; D'Amico, G. *Organometallics* **2006**, *25*, 3435–3446, and references therein.

(34) Johansson, L.; Tilset, M. *J. Am. Chem. Soc.* **2001**, *123*, 739–740.

(35) (a) Boerrigter, P. M.; te Velde, G.; Baerends, E. J. *Int. J. Quantum Chem.* **1988**, *33*, 87–113. (b) te Velde, G.; Baerends, E. J. *J. Comput. Phys.* **1992**, *99*, 84–98.

(36) Vosko, S. H.; Wilk, L.; Nusair, M. *Can. J. Phys.* **1980**, *58*, 1200–1211.

(37) Becke, A. D. *Phys. Rev.* **1988**, *A38*, 3098–3100.

(38) Perdew, J. P. *Phys. Rev.* **1986**, *B33*, 8822–8824.

scalar-relativistic zero-order regular approximation (ZORA).[39] A triple-ζ plus polarization basis set was used on platinum, the first coordination sphere atoms, and the hydrogens bound to the active carbon ligands, whereas a double-ζ plus polarization set was employed for the remaining atoms. For non-hydrogen atoms a relativistic frozen-core potential was used, including 4d for platinum, 2p for phosphorus and sulfur, and 1s for carbon, nitrogen and oxygen. A general numerical integration parameter of 5.0 was employed in all calculations. The geometries of the hypothesized minima and transition states were fully optimized at this level of theory in the gas phase. Solvation effects have been included in the gas-phase geometries by using the conductor-like screening model (COSMO) suggested by Klamt and Schuurman and implemented in ADF by Pye and Ziegler.[40] COSMO calculations were carried out by applying the default parametrization for the chloroform solvent and the following radii: Pt, 1.38 Å; C, 2.00 Å; H, 1.29 Å; O, 1.71 Å; P, 2.07 Å; S, 2.02 Å.

For the oxidative addition and reductive elimination steps, for which no transition state could be located with ADF, calculations were also performed with the Jaguar 6.0 quantum chemistry package,[41] using the same BP86 functional.[37,38] The core electrons of the platinum and phosphorus atoms were described with the Hay and Wadt core-valence relativistic effective core potential (ECP),[42] leaving the outer electrons to be treated explicitly by a basis set of double-ζ quality plus a polarization function, while all electrons were considered for remaining atoms with the 6-31G(d,p) basis set[43] (denoted as LACVP** in Jaguar). Every structure was optimized in the gas phase, and a single-point calculation was performed on the optimized structure in solution, using the Poisson–Boltzmann (PB) continuum solvent method.[44]

Vibrational frequency calculations based on analytical second derivatives at the same level of theory were carried out to confirm the local minima and transition-state geometries and to compute the zero-point energy (ZPE) and vibrational entropy corrections at 298.15 K. The unscaled vibrational energies were used to calculate the entropy correction terms using the common approximations (ideal gas, rigid rotor, and harmonic oscillator) for the partition functions. Thermal corrections for the electronic energy were also applied, and the corresponding reaction paths, in the gas phase and in chloroform, were calculated in terms of both enthalpy and free energy.

Acknowledgment. We thank the Italian Ministry for University and Research for financial support (Contract No. 2006038520).

Supporting Information Available: A table giving absolute electronic energies, thermal corrections, and entropy contributions for the considered molecules **1**–**6**, a table giving reaction and activation entropies, energies, enthalpies, and free energies for the oxidative addition and reductive elimination calculated with Jaguar, a table giving the Cartesian coordinates for the corresponding optimized geometries, a figure giving the enegy profile for the **2** to **3** oxidative addition;, and a figure giving the enegy profile for the **3** to **4** reductive elimination. This material is available free of charge via the Internet at http://pubs.acs.org.

OM701070F

(39) (a) Ziegler, T.; Tshinke, V.; Baerends, E. J.; Snijders, J. G.; Ravenek, W. *J. Phys. Chem.* **1989**, *93*, 3050–3056. (b) Li, J.; Schreckenbach, G.; Ziegler, T. *J. Am. Chem. Soc.* **1995**, *117*, 486–494, and references therein.

(40) (a) Klamt, A.; Schürmann, G. *J. Chem. Soc., Perkin Trans. 2* **1993**, 799–805. (b) Pye, C. C.; Ziegler, T. *Theor. Chem. Acc.* **1999**, *101*, 396–408.

(41) Jaguar 6.0; Schrodinger LLC, New York, 2005.

(42) Hay, P. J.; Wadt, W. R. *J. Chem. Phys.* **1985**, *82*, 299–310.

(43) Hariharan, P. C.; Pople, J. A. *Chem. Phys. Lett.* **1972**, *16*, 217–219.

(44) Tannor, D. J.; Marten, B.; Murphy, R.; Friesner, R. A.; Sitkoff, D.; Nicholls, A.; Ringnalda, M.; Goddard, W. A., III; Honig, B. *J. Am. Chem. Soc.* **1994**, *116*, 11875–11882.